Submitted to *Journal of Geophysical Research*, January 8, 2001

Ocean tidal loading effects on GPS-sensed atmospheric precipitable water vapor

Aiguo Dai
National Center for Atmospheric Research, Boulder, Colorado

Randolph H. Ware and Teresa VanHove
GPS Science & Technology Program, UCAR Office of Programs, Boulder, Colorado

Abstract

Atmospheric precipitable water vapor (PWV) derived from the Global Positioning System (GPS) has increasingly been used in atmospheric data assimilation, weather forecast, and climate studies. Ocean tides redistribute oceanic masses and can cause vertical crustal displacements in the millimeter to centimeter range at ground-based GPS sites. The effect of this displacement on GPS-sensed PWV often has not been accounted for. Here we examined this effect quantitatively using 30 min-averaged data from 53 GPS stations over North America. We find that the error due to the ocean tidal loading in short-time averaged PWV is large over the Pacific and Atlantic coastal United States (up to ±2.0–3.0 mm) and over the southern Rocky Mountains and the Gulf of Mexico (up to ±1.0–2.5 mm). This error, which increases linearly with the displacement, is smaller (within ±1.0 mm) over the Midwest and the Great Plains of the United States. Not only the displacement varies greatly from station to station, the effect of a given amount of the displacement on the PWV also differs geographically. However, the ocean loading effect on daily- and monthly-averaged PWV is small, whereas its effect on monthly-averaged diurnal cycles of the PWV can still be non-negligible at many coastal stations because the error has regular diurnal variations.

1. Introduction

The Global Positioning System (GPS) consists of a network of 24 satellites that transmit radio signals to a large number of users engaged in navigation, time transfer, and relative positioning [*Leick*, 1990]. These L-band radio signals are delayed, in part, by atmospheric water vapor (referred to as wet delay) as they travel from GPS satellites to ground-based GPS receivers. Since the early 1990s, methods have been developed to retrieve atmospheric column-integrated precipitable water vapor (PWV) using the wet delay data of GPS radio signals [e.g., *Bevis et al.*, 1992, 1994; *Rocken et al.*, 1993; *Ware et al.*, 1997]. GPS-sensed PWV is found to have an accuracy better than 2 mm [*Rocken et al.*, 1993, 1997; *Duan et al.*, 1996; *Fang et al.*, 1998; *Tregoning et al.*, 1998] at many stations, and has increasingly been used in atmospheric data assimilation, weather forecast, and climate studies [*Ware et al.*, 2000].

The errors in GPS-sensed PWV result from a number of sources, including uncertainties in determining the positions of GPS satellites and ground sites, atmospheric refraction biases [*Beutler et al.*, 1988], and the errors associated with the mapping functions to convert slant path delay into zenith path delay [*Bevis et al.*, 1994; *Fang et al.*, 1998; *Liljegren et al.*, 1999]. Variations in atmospheric pressure and ocean tides redistribute air and water masses that load the Earth's crust. The latter responds mainly by elastic deformation. Atmospheric pressure loading [*vanDam et al.*, 1994] and ocean tidal loading [*Scherneck and Haas*, 1999] can cause vertical site displacements (in the millimeter to centimeter range) at ground-based GPS sites. Although atmospheric pressure loading accounts for up to 24% of the total variance of the GPS height estimates at high-latitudes [*vanDam et al.*, 1994], its effect on the long-term (e.g., seasonal) mean of GPS-sensed PWV is likely to be small because pressure disturbances[1] are random. On the other hand, ocean tidal loading is regular (largely around diurnal and semidiurnal periods) and could potentially induce systematic biases in GPS-sensed PWV, especially on the diurnal and semidiurnal time scales [*Dai et al.*, 2000]. For example, *Shoji et al.* (2001) found that there is a semidiurnal component in the error of the GPS-sensed PWV from a Japanese GPS site and that ocean tidal loading accounts for a large part of this error. *Dragert et al.* (2000) analyzed data from a Canadian coastal GPS site and found that short-term (e.g. 3 hr) estimates of PWV can have a bias of several millimeters due to the ocean loading effect. *Dach and Dietrich* (2000) analyzed GPS data from the Antarctic Peninsula and found that the ocean loading effect can change the estimated zenith path delay by up to 10 millimeters.

The goal of this study is to quantify the effects of ocean tidal loading on GPS-sensed PWV over a large geographical domain by analyzing data from 53 GPS stations over North America. We computed the PWV using the GPS delay data twice: first without and then with ocean tidal loading. We compared the differences in the PWV and examined the effect of ocean tidal loading on instantaneous, daily mean, and daily anomaly PWV from the GPS stations. Our results show that the ocean tidal loading can induce non-negligible site displacements whose effects on the GPS-sensed PWV vary geographically. Since ocean tidal loading is not modeled explicitly and thus often excluded in the popular Bernese software [*Beutler et al.*, 1996] used to compute the GPS-sensed PWV, our results can be applied to adjust those PWV derived without ocean loading effects.

2. Data and Analysis Method

Since 1996, near real-time GPS tracking data have been obtained from a number of GPS stations operated by the NOAA Forecast Systems Laboratory and and National Geodetic Service. These data were used to derive PWV using the method described in *Bevis et al.* (1992, 1994). The Bernese v4.2 software [*Beutler et al.*, 1996] was used in this data processing. Here, we analyzed 30 min-averaged data of GPS-derived PWV for January and July 1999 and January 2000 from 53 U.S. GPS stations, which are located from Alaska to Key West, Florida (Table 1, also see Figure 3). The procedures used to derive the PWV from the GPS delay data are described in detail in *Rocken et al.* (1997), *Ware et al.* (1997), and *Dai et al.* (2000).

The long-term mean amplitudes and phases for the 11 main tidal components of the vertical displacement due to ocean tidal loading at the 53 GPS stations were provided by H.-G. Scherneck of Onsala Space Observatory, Sweden using the ocean tidal loading models described in *Scherneck and Haas* (1999). Bernese v4.2 software needs these tidal component data to calculate the vertical displacement and account for the ocean loading effect on the PWV. We used Bernese 4.2 software to calculate the vertical displacement at

[1]The regular atmospheric pressure tides are in the order of 1 mb [*Dai and Wang*, 1999] and have negligible effects.

the 53 GPS stations. The PWV was computed using the Bernese 4.2 software: first without ocean loading and then with ocean loading (using the 11 tidal components). The differences between the PWV without (PWV1) and with (PWV2) ocean loading are then examined and the regression coefficients (with PWV1 as a predictor) are computed. Since ocean tidal loading has clear diurnal and semidiurnal components, we also examined the differences in the daily mean and daily anomalies of PWV1 and PWV2.

3. Results

Figure 1 shows the time-evolution of the vertical displacement induced by ocean tidal loading and the PWV error (defined as PWV1 – PWV2) caused by the displacement for July 1999 at six GPS stations over North America. It can seen that the displacement and the PWV error have distinct diurnal cycles. The amplitude of the diurnal cycle is modulated by a near-harmonic cycle with a period around 14 days. The amplitude and phase of the displacement also vary greatly from station to station. For example, the maximum displacement is around 3.7 cm in Seattle, whereas it is only about 0.7 cm at the Stennis Island Space Center in Mississippi. The PWV error closely follows the displacement in both amplitude and phase.

Figure 2 shows that the PWV error increases linearly with the displacement. The dependence of the PWV error on the displacement weakens slightly at stations with relatively small displacements, such as at the Stennis Island Space Center where the displacement and the associated PWV error (generally within $\pm$0.5 mm) are small. This weakening of the relationship is expected as the noise becomes more significant as the signal (i.e., displacement) decreases.

The linear relationship between the PWV error and the displacement is consistent with the linear dependence of PWV on zenith wet delay [*Bevis et al.*, 1994]. It simplifies the procedure to estimate the PWV error induced by a given site displacement, which can be computed based on ocean tidal models [e.g., *Scherneck and Haas*, 1999]. We performed a linear regression using the displacement to predict the PWV error at each station. Table 1 summarizes the regression results, together with the displacement and PWV range (defined as the minimum to maximum range) found in the data.

Table 1 shows that the regression slope (b) ranges from 0.18 mm/cm at Lamont, Oklahoma to 0.69 mm/cm at Talkeetna, Alaska, whereas the intercept (a) is very close to zero. This spatial variation of b suggests that a given amount of vertical displacement can have different effects on zenith wet delay (and thus the PWV) depending on the location of the site (i.e., the partitioning of the vertical displacement into zenith wet and dry delay is location-dependent). The displacement range (in cm) varies from (–0.60, 0.65) at English Turn, Louisiana to (–3.67, 3.16) at Scripps Pier, San Diego. The PWV error range (in mm) (from the data, not from the regression equation) is smallest (–0.38, 0.22) at Clark, South Dakota and largest (–3.12, 3.13) at White Sands, New Mexico.

Figure 3 shows the spatial distribution of the displacement and PWV error range (i.e., maximum - minimum from Table 1), and the regression slope b. The locations of the GPS stations are also shown as black dots. It can be seen (Figure 3a) that the vertical displacement induced by ocean tidal loading is smallest (within $\pm$2.5/2 or 1.3 cm) over the central United States and largest (up to $\pm$3.5 cm) at stations around the Pacific coasts from Alaska to southern California. The displacement is also relatively large (within $\pm$2.0–2.5 cm) around the Atlantic coasts. Not all coastal stations, however, have large displacements. For example, stations around the Gulf of Mexico have small displacements that are comparable to those over the central inland States.

The PWV error induced by the ocean tidal loading (Figure 3b) is smallest (within $\pm$1.0 mm) over the Midwest and the Great Plains and generally larger over the Pacific and Atlantic coasts (within $\pm$2.0–3.0 mm). It is also large (within $\pm$1.0–2.5 mm) over the eastern slopes of the southern Rocky Mountains and around much of the Gulf of Mexico. It should be noticed that the displacement and PWV range shown in Table 1 and Figure 3 are the maximum range that occurred in the data of January and July 1999 and January 2000. As shown in Figure 1, the actual error at any particular time will be smaller than the range shown in Table 1 and Figure 3.

The linear regression slope b (Figure 3c) shows that for a given amount of vertical site displacement the PWV error is about twice larger around the Atlantic and Pacific coasts (b = 0.50–0.60 mm/cm) than over the central States (0.20–0.35 mm/cm). *Shoji et al.* (2001) used a value of $\sim$0.5 mm/cm for b to correct the PWV error induced by the ocean tidal loading at a Japanese GPS site. This value is comparable to the b values around the Pacific coasts in Figure 3c. Figure 3c shows that this correction coefficient varies

greatly for different locations and tends to be larger around coastal regions than over inland areas.

The PWV error ranges shown in Table 1 and Figures 2 and 3b, which are non-negligible, are for 30 min-averaged PWV. As shown by Figure 1, the PWV error concentrates mostly around the diurnal frequency. One would, therefore, expect that the PWV error to be much smaller in daily- and monthly-averaged PWV since most of the instantaneous PWV error will be cancelled out in the averaging. This is indeed the case, as shown by Figure 4. Figure 4 shows that differences between daily-averaged PWV1 and PWV2 are small (<1 mm or a few percentages) and appears to be non-systematic. These results suggest that the ocean tidal loading has a negligible effect on the mean PWV averaged over 24-hr or longer time periods.

On the other hand, the PWV error can have substantial effects on the diurnal variations of the PWV because the error has regular diurnal variations (cf. Figure 1). Figure 5 shows that the ocean tidal loading can have non-negligible effects on monthly-averaged diurnal cycles. For example, the diurnal anomaly can differ by up to 1 mm (comparable to the diurnal amplitude) at Glennallen, Alaska (Figure 5). This effect, however, is significant only at stations with relatively large site displacements. The diurnal anomalies with and without the ocean loading differ only slightly at stations with small site displacements (e.g., at the Stennis Island Space Center and Platteville, Colorado) (Figure 5).

4. Summary

We investigated the quantitative effect of ocean tidal loading on GPS-sensed PWV by analyzing 30 min-averaged data of GPS-derived PWV for January and July 1999 and January 2000 from 53 GPS stations over North America. We derived the PWV twice: first without the ocean tidal loading and then with the loading. We then examined the differences between these two kinds of PWV and their dependence on geographical locations and averaging time periods.

We find that the vertical site displacement due to the ocean tidal loading is relatively small (within ±1.3 cm) over the central United States (including coastal areas around the Gulf of Mexico) and large over the Pacific coast from Alaska to southern California (within ±3.5 cm) and over the Atlantic coastal United States (within ±2.0-2.5 cm). This site displacement induces an PWV error in the 30 min-averaged data within ±1.0 mm over the Midwest and the Great Plains of the United States. This error is much larger over the Pacific and Atlantic coastal United States (within ±2.0–3.0 mm) and over the southern Rocky Mountains and the Gulf of Mexico (within ±1.0–2.5 mm).

The PWV error due to the ocean loading has a linear dependence on the vertical displacement induced by the ocean loading. Linear regressions between these two (with the displacement as the predictor) show that the intercept is very close to zero, whereas the slope has large geographical variations with the largest values (0.50-0.60 mm/cm) over the Atlantic and Pacific coasts and the smallest values (0.20-0.35 mm/cm) over the central United States. These results suggest that the partitioning of the vertical site displacement caused by the ocean tidal loading into zenith wet and dry delay varies with location.

While the error in the short-time averaged PWV data induced by the ocean tidal loading is significant and non-negligible at many coastal stations, the ocean loading effect is negligible (<1 mm) in daily- and monthly-averaged PWV data. However, the ocean loading has significant effects (up to 1 mm, comparable to the diurnal amplitude) on monthly-averaged diurnal cycles at many coastal stations.

Our results suggest that the effect of ocean tidal loading can induce significant errors which could be a substantial part of the rms error of GPS-sensed PWV in validation studies [e.g., *Rocken et al.*, 1993, 1997; *Duan et al.*, 1996; *Fang et al.*, 1998; *Tregoning et al.*, 1998; *Lijegren et al., 1999*; *Shoji et al.*, 2001]. This is especially true for stations over many coastal regions. Furthermore, our results show that not only the site displacement induced by the ocean tidal loading varies greatly from location to location, the effect of a given amount of the displacement on the GPS-sensed PWV also differs geographically. Thus, we strongly recommend to use ocean tidal models to compute the site displacement for individual stations and include it in the PWV calculation.

Acknowledgments. We are grateful to Hans-Georg Scherneck of Onsala Space Observatory, Sweden for calculating the leading tidal components of displacement at the 53 GPS stations. This work was supported by a NOAA small grant (grant no. NA87GP0105) and an NSF small grant on GPS-sensed precipitable water. The National Center for Atmospheric Research is sponsored by the National Science Foundation.

References

Beutler, G., I. Bauersima, W. Gurtner, M. Rothacher, T. Schildknecht, and A. Geiger, Atmospheric refraction and other important biases in GPS carrier phase observations, In: *Atmospheric Effects on Geodetic Space Measurements*, *Monograph 12*, F.K. Brunner (ed.), School of Surveying, University of New South Wales, pp. 15-43, 1988.

Beutler, G., E. Brockmann, S. Fankhauser, W. Gurtner, J. Johnson, L. Mervart, M. Rothacher, S. Schaer, T. Springer, and R. Weber, *Bernese GPS Software Version 4.0 Documenation*, 1996.

Bevis, M., S. Businger, T.A. Herring, C. Rocken, R.A. Anthes, and R.H. Ware, GPS meteorology: Remote sensing of atmospheric water vapor using the Global Positioning System, *J. Geophys. Res., 97*, 15,787-15,801, 1992.

Bevis, M., S. Businger, S, Chiswell, T.A. Herring, R. Anthes, C. Rocken, and R.H. Ware, GPS meteorology: Mapping zenith wet deplays onto precipitable water, *J. Appl. Meteor., 33*, 379-386, 1994.

Dach, R. and R. Dietrich, Influence of the ocean loading effect on GPS derived precipitable water vapor, *Geophys. Res. Lett., 27*, 2953-2958, 2000.

Dai, A., and J. Wang, Diurnal and semidiurnal tides in global surface pressure fields, *J. Atmos. Sci., 56*, 3874-3891, 1999.

Dai, A., J. Wang, R.H. Ware, and T. Van Hove, Diurnal variation in atmospheric water vapor over North America and its implications for sampling errors in radiosonde humidity, to be submitted to *J. Geophys. Res.*, 2000.

Dragert, H., T.S. James, and A. Lambert, Ocean loading corrections for continuous GPS: A case study at the Canadan Coastal site Holberg, *Geophys. Res. Lett., 27*, 2045-2048, 2000.

Duan, J., M. Bevis, P. Fang, Y. Bock, S. Chiswell, S. Businger, C. Rocken, F. Solheim, T. Van Hove, R. Ware, S. McClusky, T.A. Herring, and R.W. King, GPS meteorology: direct estimation of the absolute value of precipitable water, *J. Appl. Meteor., 35*, 830-838, 1996.

Fang, P., M. Bevis, Y. Bock, S. Gutman, and D. Wolfe, GPS meteorology: Reducing systematic errors in geodetic estimates for zenith delay, *Geophys. Res. Lett., 25*, 3583-3586, 1998.

Leick, A., *GPS Satellite Surveying.* John Wiley and Sons, 353pp., 1990.

Lijegren, J., B. Lesht, T. Van Hove, and C. Rocken, A comparison of integrated water vapor from microwave radiometer, balloon-borne sounding system and Global Positioning System, paper presented at *the 9th Atmospheric Radiation Measurements (ARM) meeting*, San Antonia, Texas, 22-26 March, 1999.

Rocken, C., R. Ware, T. Van Hove, F. Solheim, C. Alber, and J. Johnson, Sensing atmospheric water vapor with the Global Positioning System, *Geophys. Res. Lett., 20*, 2631-2634, 1993.

Rocken, C., T. Van Hove, amd R. Ware, Near real-time GPS sensing of atmospheric water vapor, *Geophys. Res. Lett., 24*, 3221-3224, 1997.

Scherneck, H.-G. and R. Haas, Effect of horizontal displacements due to ocean tide loading on the determination of polar motion and UT1, *Geophys. Res. Lett., 26*, 501-504, 1999.

Shoji, Y., H. Nakamura, K. Aonashi, A. Ichiki, and H. Seko, Semidiurnal variation of the errors of GPS precipitable water vapor caused by site displacement due to ocean tidal loading. *Earth, Planets & Space*, in press, 2001.

Tregoning, P., R. Boers, D. O'Brien, and M. Hendy, Accuracy of absolute precipitable water vapor estimates from GPS observations, *J. Geophys. Res., 103*, 28,701-28,710, 1998.

vanDam, T.M., G. Blewitt, and M.B. Heflin, Atmospheric pressure loading effects on Global Positioning System coordinate determinations, *J. Geophys. Res., 99*, 23,939-23,950, 1994.

Ware, R.H., C. Alber, C. Rocken, and F. Solheim, Sensing integrated water vapor along GPS ray paths, *Geophys. Res. Lett., 24*, 417-420, 1997.

Ware, R.H., D.W. Fulker, S.A. Stein, D.N. Anderson, S.K. Avery, R.D. Clark, K.K. Droegemeier, J.P. Kuettner, J.B. Minster, S. Sorooshian, SuomiNet: a real-time national GPS network for atmospheric research and education, *Bull. Am. Meteorol. Soc., 81*, 677-694, 2000.

Address of all authors: P.O. Box 3000, Boulder, CO 80307 (email for A. Dai: adai@ucar.edu)

This preprint was prepared with AGU's LaTeX macros v5.01. File ocean-loading-paper formatted January 8, 2001.

Table 1: Station locations, regressional coefficients [PWV_error (mm) = a + b*Displacement(cm)], the vertical displacement range, and PWV error range derived using data for January and July 1999 and January 2000.

No.	Stn.	(long, lat.)	(a, b)	Displ_range	PWV_E_range	Location
1	NLGN	(-97.8, 42.2)	(0.00, 0.29)	(-1.00, 1.12)	(-0.47, 0.50)	Neligh, Nebraska
2	SLAI	(-93.7, 41.9)	(0.00, 0.22)	(-0.99, 1.00)	(-0.33, 0.37)	Slater, Iowa
3	LMNO	(-97.5, 36.7)	(0.00, 0.18)	(-0.62, 1.20)	(-1.83, 1.40)	Lamont, Oklahoma
4	AZCN	(-107.9, 36.8)	(0.03, 0.29)	(-1.20, 1.26)	(-1.58, 2.77)	Aztec, New Mexico
5	BLKV	(-80.4, 37.2)		(-1.40, 1.10)	(-0.43, 0.44)	Blacksburg, Virginia
6	BLMM	(-90.0, 36.9)	(0.00, 0.32)	(-1.03, 0.92)	(-0.77, 0.45)	Bloomfield, Missouri
7	BLRW	(-90.5, 43.2)	(0.01, 0.24)	(-1.04, 0.98)	(-0.39, 0.37)	Blue River, Wisconsin
8	CENA	(-144.7, 65.5)	(-0.04, 0.59)	(-1.98, 2.12)	(-2.02, 1.73)	Central, Alaska
9	CNWM	(-92.7, 37.5)	(0.01, 0.29)	(-1.00, 0.94)	(-0.50, 0.41)	Conway, Missouri
10	DQUA	(-94.3, 34.1)	(-0.01, 0.25)	(-0.93, 0.88)	(-1.38, 0.84)	Dequeen, Arkansas
11	FBYN	(-97.3, 40.1)	(0.00, 0.27)	(-1.00, 1.07)	(-0.44, 0.49)	Fairbury, Nebraska
12	GDAC	(-102.2, 37.8)	(0.00, 0.30)	(-1.05, 1.15)	(-1.47, 0.83)	Granada, Colorado
13	GNAA	(-146.0, 62.1)	(-0.03, 0.63)	(-3.06, 3.44)	(-2.56, 2.98)	Glennallen, Alaska
14	HBRK	(-97.3, 38.3)	(0.00, 0.27)	(-1.01, 1.05)	(-0.59, 0.47)	Hillboro, Kansas
15	HKLO	(-95.9, 35.7)	(0.00, 0.26)	(-0.97, 0.95)	(-1.22, 0.91)	Haskell, Oklahoma
16	HVLK	(-99.1, 37.7)	(-0.01, 0.26)	(-1.01, 1.07)	(-1.76, 0.92)	Haviland, Oklahoma
17	JTNT	(-101.0, 33.0)	(0.00, 0.26)	(-1.03, 0.96)	(-1.03, 0.81)	Jayton, Texas
18	LTHM	(-94.2, 39.6)	(0.00, 0.27)	(-1.01, 1.00)	(-0.48, 0.41)	Lathrop, Missouri
19	MBWW	(-106.2, 41.9)	(-0.02, 0.32)	(-1.03, 1.40)	(-2.54, 0.76)	Medicine Bow, Wyoming
20	MRRN	(-101.7, 42.9)	(0.00, 0.30)	(-1.00, 1.25)	(-0.54, 0.70)	Merriman, Nebraska
21	NDBC	(-89.6, 30.4)	(0.00, 0.38)	(-0.66, 0.61)	(-1.17, 1.10)	Stennis Is.Space Ctr,MS
22	NDSK	(-95.6, 37.4)	(0.00, 0.25)	(-1.00, 1.00)	(-1.49, 1.36)	Neodesha, Nebraska
23	OKOM	(-88.9, 34.1)	(0.02, 0.25)	(-0.97, 0.83)	(-0.46, 0.51)	Okolona, Missippi
24	PATT	(-95.7, 31.8)	(0.00, 0.20)	(-0.82, 0.77)	(-0.96, 1.01)	Palestine, Texas
25	PLTC	(-104.7, 40.2)	(-0.01, 0.29)	(-1.07, 1.31)	(-1.43, 0.73)	Platteville, Colorado
26	PRCO	(-97.5, 35.0)	(0.00, 0.25)	(-0.97, 0.96)	(-0.61, 0.51)	Purcell, Oklahoma
27	RWDN	(-100.7, 40.1)	(0.00, 0.30)	(-1.00, 1.15)	(-0.52, 0.61)	McCook, Nebraska
28	SEAW	(-122.3, 47.7)	(0.01, 0.50)	(-2.48, 3.77)	(-1.92, 2.90)	Seattle, Washington
29	SIO3	(-117.3, 32.9)	(0.01, 0.46)	(-3.67, 3.16)	(-2.75, 2.14)	Scripps Pier, San Diego
30	SYCN	(-76.1, 43.1)	(0.01, 0.37)	(-1.47, 1.03)	(-0.71, 0.67)	Syracuse, New York
31	TCUN	(-103.6, 35.1)	(0.01, 0.30)	(-1.12, 1.10)	(-1.21, 2.46)	Tucumcari, New Mexico
32	TLKA	(-150.4, 62.3)	(0.00, 0.69)	(-2.87, 3.03)	(-2.85, 3.00)	Talkeetna, Alaska
33	VCIO	(-99.2, 36.1)	(0.00, 0.29)	(-1.00, 1.02)	(-2.35, 2.73)	Vici, Oklahoma
34	WDLM	(-95.4, 44.7)	(0.00, 0.22)	(-0.99, 1.07)	(-0.42, 0.36)	Wood Lake, Minnesota
35	WLCI	(-87.1, 40.8)	(0.01, 0.30)	(-1.13, 0.96)	(-0.67, 0.42)	Wolcott, Indiana
36	WNFL	(-92.8, 31.9)	(-0.01, 0.26)	(-0.83, 0.74)	(-2.28, 2.95)	Winnfield, Louisiana
37	WSMN	(-106.3, 32.4)	(0.01, 0.38)	(-1.38, 1.08)	(-3.12, 3.13)	White Sands, New Mexico
38	CCV3	(-80.5, 28.5)	(0.00, 0.46)	(-2.27, 1.79)	(-1.41, 1.57)	Cape Canaveral, Florida
39	MOB1	(-88.0, 30.2)	(0.00, 0.32)	(-0.56, 0.73)	(-0.61, 0.75)	Mobile, Alabama
40	ARP3	(-97.1, 27.8)	(-0.02, 0.11)	(-0.45, 0.56)	(-0.91, 1.39)	Aransas Pass, Texas
41	GAL1	(-94.7, 29.3)	(-0.02, 0.45)	(-0.65, 0.73)	(-1.05, 0.93)	Galveston, Texas
42	ENG1	(-89.9, 29.9)	(0.01, 0.31)	(-0.60, 0.65)	(-1.03, 1.23)	English Turn, Louisiana
43	EKY1	(-82.8, 27.6)	(0.00, 0.37)	(-0.61, 0.70)	(-0.57, 0.84)	Egmont Key, Florida
44	MIA3	(-80.2, 25.7)	(-0.03, 0.33)	(-1.61, 1.36)	(-0.95, 0.93)	Miami, Florida
45	SHK1	(-74.0, 40.5)	(0.03, 0.56)	(-2.69, 1.88)	(-1.87, 1.99)	Sandy Hook, New Jersey
46	KYW1	(-81.7, 24.6)	(-0.02, 0.36)	(-0.71, 0.71)	(-0.62, 0.71)	Key West, Florida
47	CHA1	(-79.8, 32.8)	(0.02, 0.52)	(-2.81, 2.19)	(-1.77, 1.93)	Charleston, S. Carolina
48	FMC1	(-76.7, 34.7)	(0.01, 0.55)	(-3.06, 2.34)	(-1.82, 1.84)	Ft Macon, North Carolina
49	MOR1	(-72.7, 40.8)	(0.00, 0.61)	(-2.87, 1.96)	(-1.92, 2.07)	Moriches, New York
50	DRV1	(-76.6, 37.0)	(-0.03, 0.49)	(-1.78, 1.29)	(-1.01, 0.73)	Driver, Virginia
51	CLK1	(-98.0, 44.9)	(-0.04, 0.15)	(-0.98, 1.14)	(-0.38, 0.22)	Clark, South Dakota
52	WHN1	(-103.3, 42.7)	(-0.02, 0.23)	(-1.01, 1.30)	(-0.60, 0.68)	Whitney, Nebraska
53	SAV1	(-81.7, 32.1)	(0.00, 0.51)	(-1.85, 1.43)	(-1.20, 1.40)	Savannah, Georgia

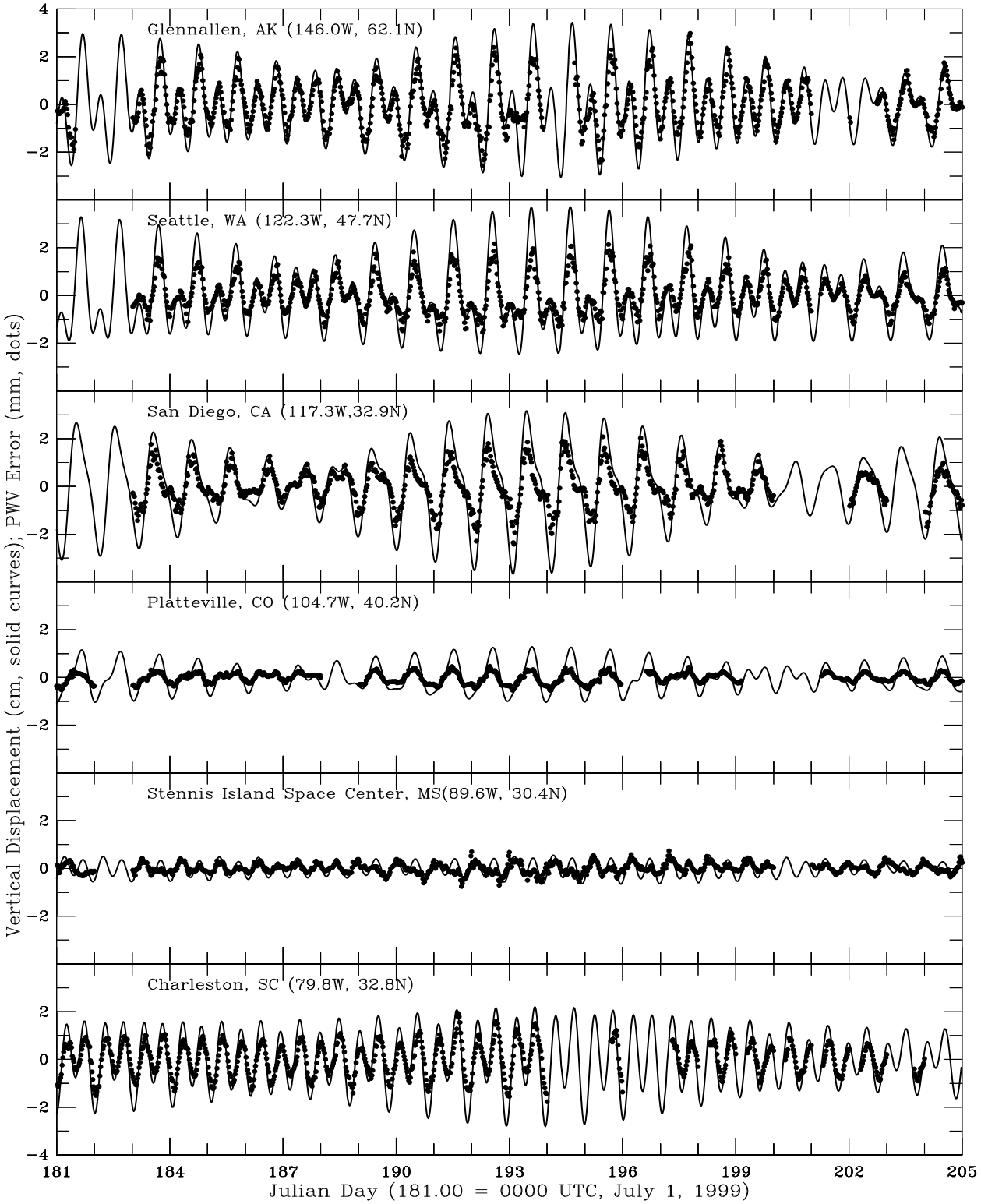

Figure 1. Vertical displacements (cm, solid curves) induced by ocean tidal loading and the PWV error (mm, dots; defined as PWV without ocean loading minus PWV with ocean loading) caused by the displacement for July 1999 at six GPS stations.

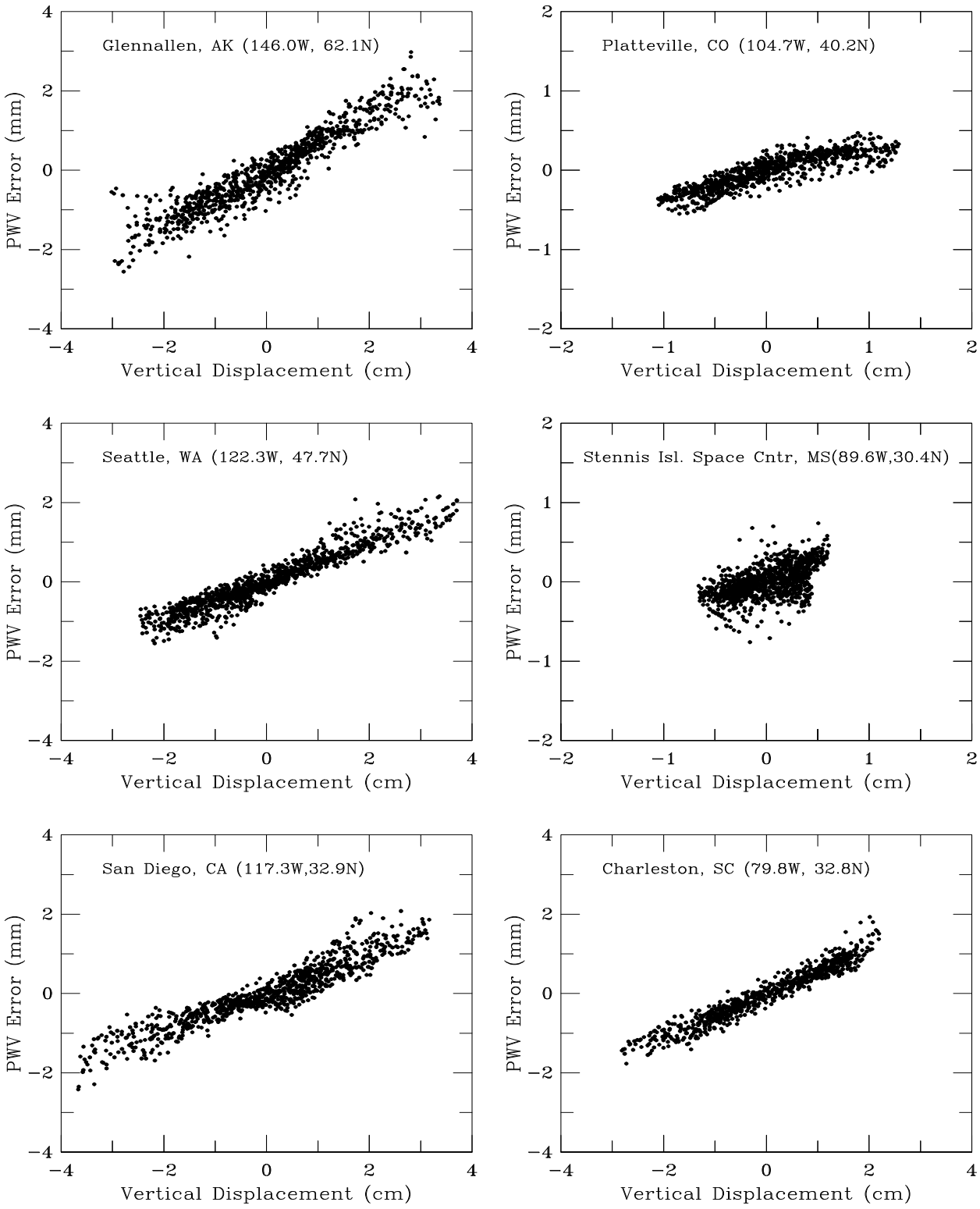

Figure 2. Scatter plots of the displacement and PWV error shown in Figure 1.

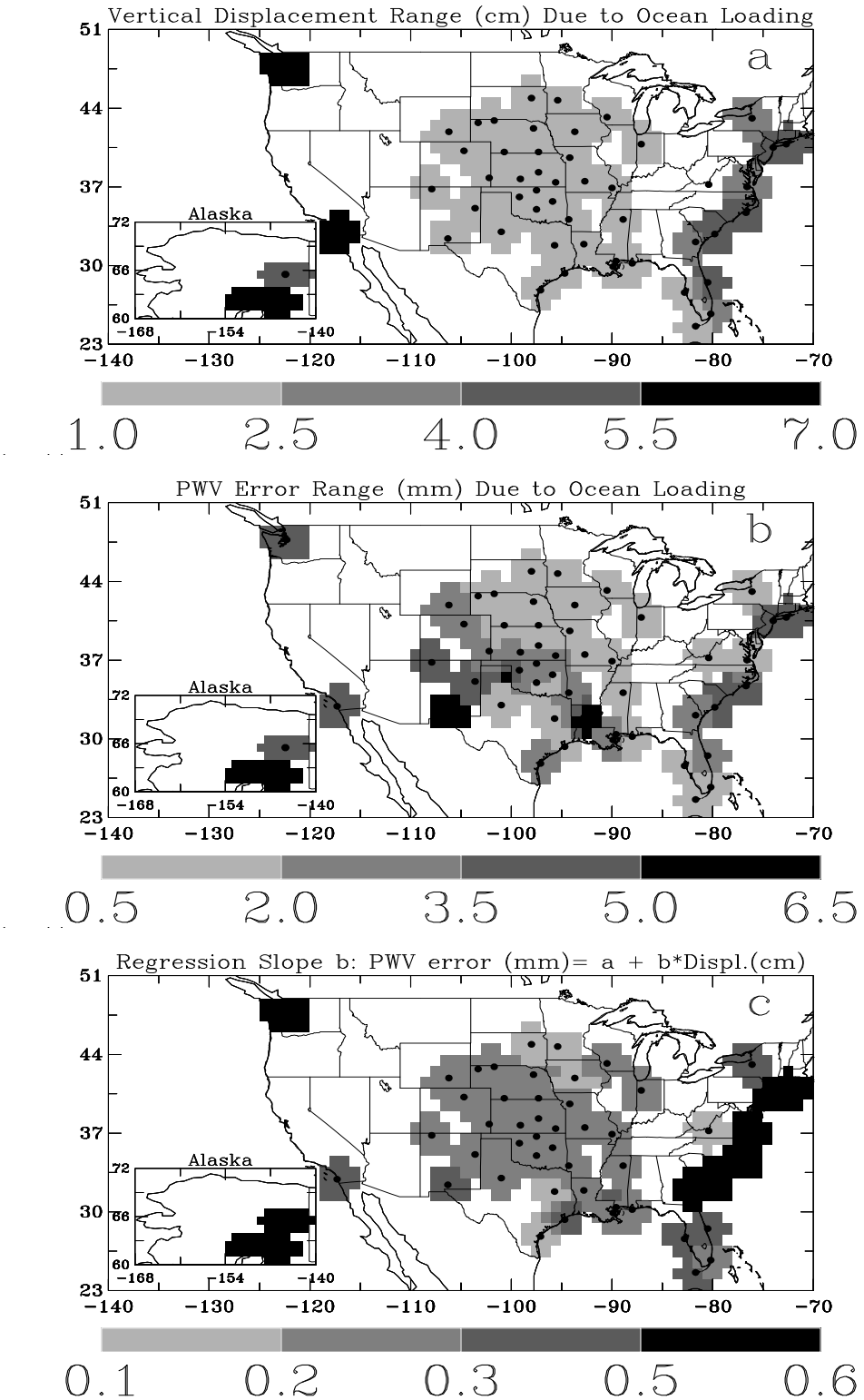

Figure 3. **a**. Spatial distribution of the vertical displacement range (cm), **b**. PWV error range (mm), and **c**. regression slope b (mm/cm) listed in Table 1. The dots indicate locations of the 53 GPS stations.

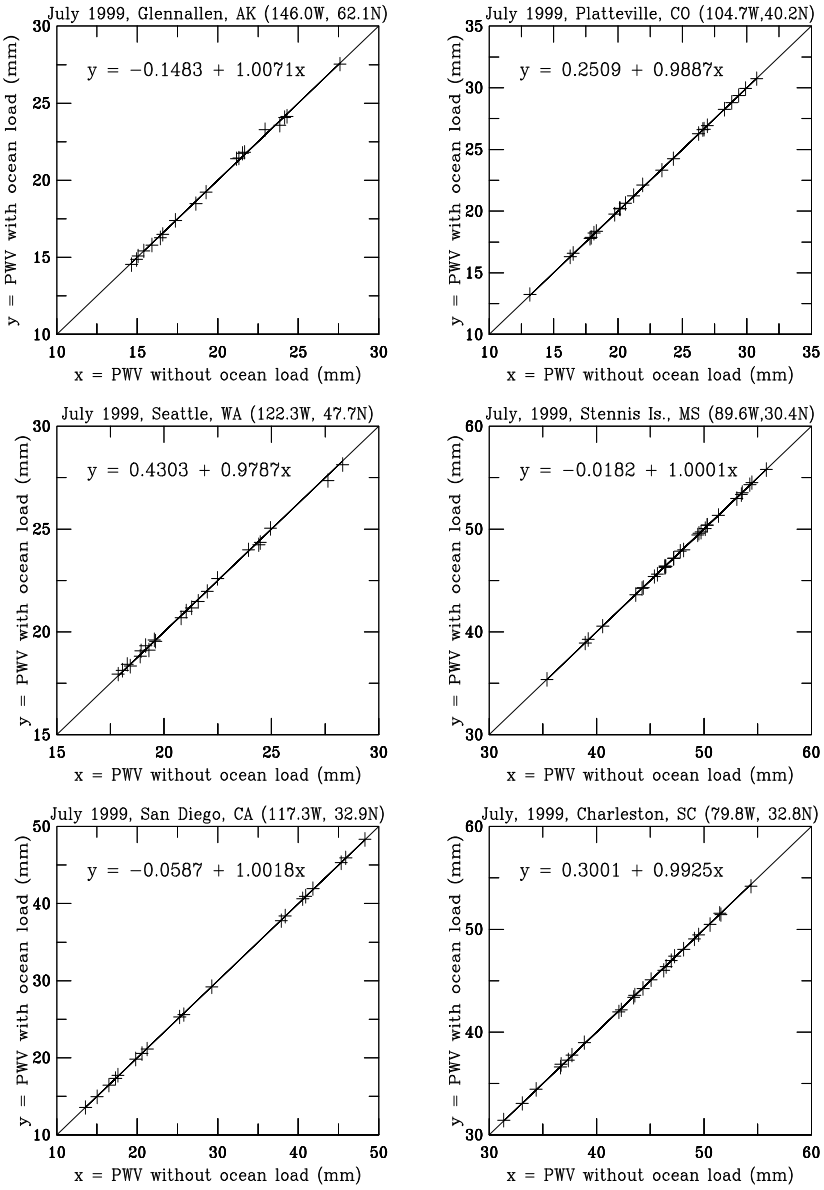

Figure 4. Scatter plots of the daily mean PWV (mm) derived with and without ocean loading for July 1999 at six GPS stations. The straight line is for the x=y case.

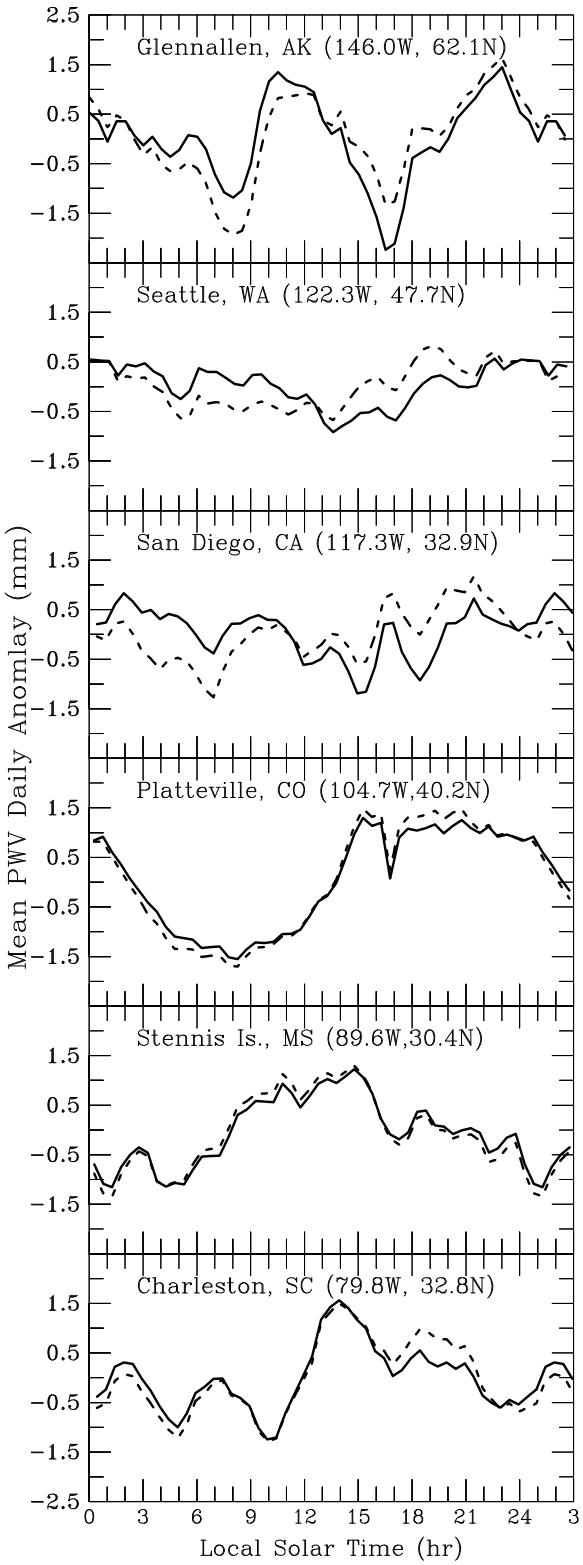

Figure 5. Mean diurnal evolution of PWV derived with (dashed curves) and without (solid curves) ocean loading for July 1999 at six GPS stations.